

Discussing the Relationship between the Static and Dynamic Light Scattering

Yong Sun

November 10, 2019

Abstract

Both the static (*SLS*) and dynamic (*DLS*) light scatterings obtain the information from the scattered intensity, but the size information is different. In this paper, the relationship between SLS and DLS is discussed based on dilute water dispersions of two different homogenous spherical particles, polystyrene latexes and poly(*N*-isopropylacrylamide) microgels, with a simple assumption when Rayleigh-Gans-Debye approximation is valid. With the assistance of the simulated data, what the apparent hydrodynamic radius means has been discussed. The results show that the apparent hydrodynamic radius is different with the mean hydrodynamic radius of particles and is a composite size obtained from averaging the term $\exp(-q^2 D\tau)$ in the static size distribution $G(R_s)$ with the weight $R_s^6 P(q, R_s)$.

In general, the structural information and mass weight are included in the relationship between the average scattered intensity and the scattering angle. Measuring this dependence is called the static light scattering (*SLS*). The analysis of the time auto-correlation of the scattered intensity can provide the dynamic information of particles, called the dynamic light scattering (*DLS*). SLS obtains the information from the optical feature and DLS gains the information from both the optical and hydrodynamic characteristics of particles. If the relationship between the optical and hydrodynamic features of particles can be built, the experimental information of the normalized time auto-correlation function of the intensity of the scattered light $g^{(2)}(\tau)$ can be expected by using the size information obtained from SLS. In this article, the relationship between the SLS and DLS for homogenous spherical particles will be discussed with a simple assumption when Rayleigh-Gans-Debye (*RGD*) approximation is valid.

For homogeneous spherical particles where the RGD approximation is valid, the normalized time auto-correlation function of the electric field of the scattered light $g^{(1)}(\tau)$ is given by

$$g^{(1)}(\tau) = \frac{\int_0^\infty R_s^6 P(q, R_s) G(R_s) \exp(-q^2 D\tau) dR_s}{\int_0^\infty R_s^6 P(q, R_s) G(R_s) dR_s}, \quad (1)$$

where q is the scattering vector, R_s is the static radius, τ is the delay time, D is the diffusion coefficient, $G(R_s)$ is the number distribution and the form factor $P(q, R_s)$ is

$$P(q, R_s) = \frac{9}{q^6 R_s^6} (\sin(qR_s) - qR_s \cos(qR_s))^2. \quad (2)$$

In this discussion, the number distribution is chosen as a Gaussian distribution

$$G(R_s; \langle R_s \rangle, \sigma) = \frac{1}{\sigma \sqrt{2\pi}} \exp \left(-\frac{1}{2} \left(\frac{R_s - \langle R_s \rangle}{\sigma} \right)^2 \right),$$

where $\langle R_s \rangle$ is the mean static radius and σ is the standard deviation relative to the mean static radius.

From the Stokes-Einstein relation

$$D = \frac{k_B T}{6\pi\eta_0 R_h},$$

here η_0 , k_B , T and R_h are the viscosity of the solvent, Boltzmann's constant, absolute temperature and hydrodynamic radius of a particle.

If we simply assume that the relationship between the static and hydrodynamic radii is given by

$$R_h = aR_s, \quad (3)$$

where a is a constant, with the function between the normalized time auto-correlation function of the intensity of the scattered light $g^{(2)}(\tau)$ and the normalized time auto-correlation function of the electric field of the scattered light $g^{(1)}(\tau)$ [1]

$$g^{(2)}(\tau) - 1 = \beta \left(g^{(1)} \right)^2, \quad (4)$$

the relationship between the static and dynamic light scattering is built and the values of the normalized time auto-correlation function of the intensity of the scattered light $g^{(2)}(\tau)$ can be expected.

In this paper, the calculated and experimental values of $g^{(2)}(\tau)$ of two samples were compared. One is the polystyrene latex sample with the normalized size information: the mean radius is 33.5 nm and the standard deviation is 2.5 nm provided by the supplier, from Interfacial Dynamics Corporation (Portland, Oregon). The other is the poly(*N*-isopropylacrylamide) (PNIPAM) microgel sample with the molar ratio 1% of crosslinker *N,N'*-methylenebisacrylamide over *N*-isopropylacrylamide. The size information was obtained by fitting the static light scattering. At the temperature 29°C, the mean static radius is 254.3±0.1nm, the standard deviation is 21.5±0.3nm and χ^2 is 2.15 [2].

If the constant a for the polystyrene latex sample is assumed to be 1.1 and the size information provided by the supplier is thought to be consistent with that obtained from SLS, all the experimental and calculated values of $g^{(2)}(\tau)$ at the scattering angles 30°, 60°, 90°, 120° and 150° are shown in Fig. 1.a.

When the constant a for the PNIPAM sample is assumed to be 1.21, all the experimental and calculated values at the scattering angles 30°, 50° and 70° are shown in Fig. 1.b. Figure 1 shows that the calculated values are consistent with the experimental data very well.

If the static radius is thought to be equal to the hydrodynamic radius as Bargeron think [3], all the experimental and calculated values of $g^{(2)}(\tau)$ for the polystyrene latex sample at the scattering angles 30°, 60°, 90°, 120° and 150° are shown in Fig. 2.a; all the experimental and calculated values for the PNIPAM sample at the scattering angles 30°, 50° and 70° are shown in Fig. 2.b. Figure 2 shows that the expected values have large differences with the experimental data.

Traditionally the size information is obtained from DLS. The standard method is the Cumulant or the inverse Laplace transform. For the five experimental data of $g^{(2)}(\tau)$ measured under the same conditions with the SLS data, the five fit results of $g^{(2)}(\tau)$ by using the first Cumulant and first two Cumulant [4, 5] respectively for the PNIPAM microgel sample at temperature 29°C and the scattering angle 30° are listed in Table 1.

	$\langle \Gamma \rangle_{first}$	χ^2	$\langle \Gamma \rangle_{two}$	μ_2	χ^2
1	79.5 ± 0.1	0.07	79.9 ± 0.3	28.20 ± 15.99	0.04
2	79.0 ± 0.1	0.33	80.4 ± 0.3	90.10 ± 17.11	0.04
3	79.7 ± 0.1	0.11	80.3 ± 0.3	39.17 ± 16.19	0.05
4	79.4 ± 0.1	0.07	79.7 ± 0.3	20.93 ± 15.92	0.06
5	78.7 ± 0.1	0.53	80.4 ± 0.3	112.75 ± 17.26	0.08

Table 1 The fit results for the PNIPAM sample at temperature 29°C and the scattering angle 30°.

From the fit results, the values of the mean decay constant $\langle \Gamma \rangle$ show the independence on the measurements, but the results of μ_2 have a strong dependence on the measurements. The values of μ_2 are often negative. It's a contradiction with its definition. In order to discuss this problem conveniently, the simulated data will be used.

The simulated data were produced by using the size information: the mean static radius is 260 nm and the standard deviation is 26 nm. the temperature T was set to 302.33K, the viscosity of the solvent η_0 was 0.8132 mPa S, the scattering angle was 30° and the constant a was chosen as 1.2. When the data of $(g^{(2)}(\tau) - 1) / \beta$ was obtained, the 1% statistical noise was added and the random errors were set 3%. Five simulated data were produced respectively. The fit results of the five simulated data by using the first Cumulant and first two Cumulant respectively are shown in Table 2.

	$\langle \Gamma \rangle_{first}$	χ^2	$\langle \Gamma \rangle_{two}$	μ_2	χ^2
1	79.27 ± 0.01	11.98	79.90 ± 0.02	22.0 ± 0.6	7.75
2	78.50 ± 0.01	4.56	78.98 ± 0.03	9.8 ± 0.6	3.83
3	78.35 ± 0.01	5.67	79.43 ± 0.06	20.6 ± 1.2	4.66
4	78.33 ± 0.01	25.40	78.25 ± 0.02	-1.7 ± 0.4	25.44
5	78.596 ± 0.004	15.75	78.79 ± 0.02	4.9 ± 0.5	15.55

Table 2 The fit results for the simulated data with the standard deviation 26 nm.

From the fit results of the simulated data that are shown in Table 2, the situation is the same with the real experimental data, the values of the mean decay constant $\langle \Gamma \rangle$ show the independence on the different noises and errors and the results of μ_2 have strong dependences on them. The values of μ_2 can be negative. As we have discussed, a truncated Gaussian distribution can give better results for the static light scattering of the PNIPAM sample at temperature 29°C [2], so the five simulated data were produced respectively again with the truncated Gaussian distribution that the range of integral was 221 to 299 nm. The fit results of the five simulated data by using the first Cumulant and first two Cumulant respectively are shown in Table 3. The conclusion is the same that the values of the quantity μ_2 have large differences for different simulated data and are often negative.

	$\langle \Gamma \rangle_{first}$	χ^2	$\langle \Gamma \rangle_{two}$	μ_2	χ^2
1	79.996 ± 0.002	10.96	79.73 ± 0.02	-5.4 ± 0.4	10.36
2	79.83 ± 0.01	20.57	79.79 ± 0.05	-0.95 ± 1.24	20.63
3	80.091 ± 0.004	5.30	80.69 ± 0.04	12.8 ± 0.8	4.61
4	79.926 ± 0.009	3.97	80.14 ± 0.03	4.3 ± 0.6	3.84
5	79.985 ± 0.005	9.00	80.48 ± 0.02	9.4 ± 0.3	5.51

Table 3 The fit results for the simulated data with the truncated distribution.

Comparing the fit results by using the first Cumulant with the values by using the first two Cumulant for the experimental and simulated data, the values of the mean decay constant can be thought to be equal. In order to avoid the contradiction that the values of μ_2 are often negative, the apparent hydrodynamic radius is obtained by using the first Cumulant. Meanwhile from the analysis of Cumulant method, the apparent hydrodynamic radius is obtained from the average of the term $\exp(-q^2 D\tau)$ in distribution $G(R_s)$ with the weight $R_s^6 P(q, R_s)$. In order to explore the effects of the distribution, the simulated data were produced as the above simulated data with the same mean static radius 260 nm and the different standard deviations 13, 39 and 52 nm respectively. The constant a is still chosen 1.2. From this assumption, the mean hydrodynamic radius should be 312 nm. The fit results for different standard deviations are listed in Table 4.

$\sigma / \langle R_s \rangle$	R_h (nm)
5%	315.7 ± 0.9
10%	$325. \pm 2.$
15%	339.4 ± 0.9
20%	$356. \pm 1.$

Table 4 The apparent hydrodynamic radii of the simulated data produced by using the same mean static radius and different standard deviations.

From the results of apparent hydrodynamic radius, the values are apparently affected by the values of standard deviation. As shown in Eq. 1, the quantity $\exp(-q^2 D\tau)$ is determined by the hydrodynamic feature of particles while $R_s^6 P(q, R_s)$ is determined by the optical feature of particles. As a result,

$g^{(2)}(\tau)$ is determined by both the optical and hydrodynamic characteristics. When the Cumulant method is used, the apparent hydrodynamic radius R_h obtain from the normalized time auto-correlation function of the intensity of the scattered light $g^{(2)}(\tau)$ is a composite size. If the simple size information need to be obtained from $g^{(2)}(\tau)$, the relation between the optical and hydrodynamic features of particles must be considered. The accurate relationship between the static and hydrodynamic radii can be further explored.

Fig. 1 The expected and experimental values of the normalized time auto-correlation function of the intensity of the scattered light $g^{(2)}(\tau)$. Figures 1.a and 1.b show the results of the polystrene latex and PNIPAM samples respectively. The symbols show the experimental results and the line shows the calculated values with the simple assumption $R_h = aR_s$.

Fig. 2. The expected and experimental values of the normalized time auto-correlation function of the intensity of the scattered light $g^{(2)}(\tau)$. Figures 2.a and 2.b show the results of the polystrene latex and PNIPAM samples respectively. The symbols show the experimental results and the line shows the calculated values with the simple assumption $R_h = R_s$.

[1] P. N. Pusey in Neutrons, X-rays and Light: Scattering Methods Applied to Soft Condensed Matter, edited by P. Lindner and Th. Zemb, Elsevier Science B.V., Amsterdam, The Netherlands, 2002.

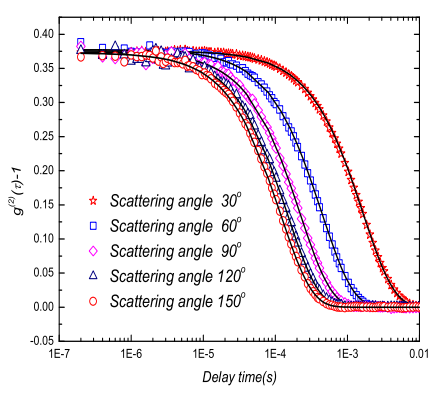
[2] Y. Sun, Unpublished (please see my second paper)

[3] C. B. Barger, J. Chem. Phys. 1974, 61, 2134.

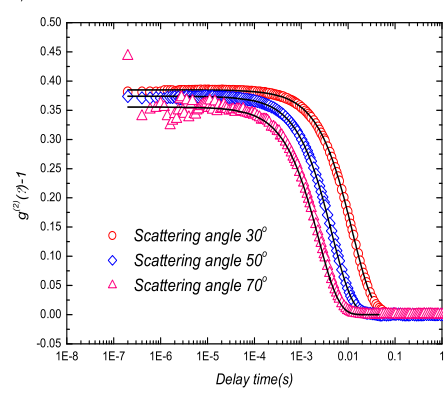
[4] B. J. Berne and R. Pecora, Dynamic Light Scattering, Robert E. Krieger Publishing Company, Malabar, Florida, 1990.

[5] J. C. Brown, P. N. Pusey, R. Dietz, J. Chem. Phys. 1975, 62, 1136.

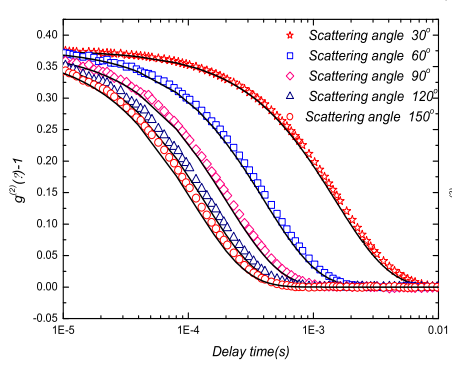
1). a



1). b



2). a



2). b

